Parameters Involved in Antimicrobial and Endotoxin Detoxification Activities of Antimicrobial Peptides[†]

Yosef Rosenfeld,[‡] Hans-Georg Sahl,[§] and Yechiel Shai*[,‡]

Department of Biological Chemistry, The Weizmann Institute of Science, Rehovot, 76100 Israel, and Institute for Medical Microbiology, Immunology and Parasitology, Pharmaceutical Microbiology Section, University of Bonn, Sigmund-Freud-Strasse 25, D-53127 Bonn, Germany

Received March 17, 2008; Revised Manuscript Received April 21, 2008

ABSTRACT: Endotoxin [lipopolysaccharide (LPS)] covers more than 90% of the outer monolayer of the outer membrane of Gram-negative bacteria, and it plays a dual role in its pathogenesis: as a protective barrier against antibiotics and as an effector molecule, which is recognized by and activates the innate immune system. The ability of host-defense antimicrobial peptides to bind LPS on intact bacteria and in suspension has been implicated in their antimicrobial and LPS detoxification activities. However, the mechanisms involved and the properties of the peptides that enable them to traverse the LPS barrier or to neutralize LPS endotoxic activity are not yet fully understood. Here we investigated a series of antimicrobial peptides and their analogues with drastically altered sequences and structures, all of which share the same amino acid composition (K_6L_9). The list includes both all-L-amino acid peptides and their diastereomers (composed of both L- and D-amino acids). The peptides were investigated functionally for their antibacterial activity and their ability to block LPS-dependent TNF-α secretion by macrophages. Fluorescence spectroscopy and transmission electron microscopy were used to detect their ability to bind LPS and to affect its oligomeric state. Their secondary structure was characterized in solution, in LPS suspension, and in LPS multibilayers by using CD and FTIR spectroscopy. Our data reveal specific biophysical properties of the peptides that are required to kill bacteria and/or to detoxify LPS. Besides shedding light on the mechanisms of these two important functions, the information gathered should assist in the development of AMPs with potent antimicrobial and LPS detoxification activities.

Endotoxin [lipopolysaccharide (LPS)][1] plays a dual role in Gram-negative bacteria pathogenesis: as one of the barriers, by defending the bacteria from their surroundings, and as an effector molecule, by initiating immune response against the invading bacteria (*1*). LPS covers more than 90% of the outer monolayer of the outer membrane of Gram-negative bacteria, creating the first permeability barrier that makes this membrane relatively impermeable to hydrophobic antibiotics, detergents, and host proteins (*2*). Mode of action studies suggest two mechanisms that explain the function of LPS as a permeability barrier (*2*). The first states that the barrier properties of LPS are mediated through its saccharidic portion, which acts as a hydrophilic shield that prevents the passage of hydrophobic molecules (*3*). The second hypothesis states that a series of intermolecular links form a cross bridge with divalent cations and by that mechanism tightly link LPS molecules in the outer membrane to form an impenetrable barrier (*4*).

Upon being shed from bacteria as a consequence of cell division, death, or antibiotic treatment (*5*), LPS forms oligomers in suspension that are recognized as a pathogen-associated molecular pattern (PAMP) by innate immune cells (*6*). This process of recognition involves binding of LPS to serum proteins [such as LPS-binding protein (LBP)] (*7*) followed by binding to membrane-bound proteins (CD14 and TLR-4). This initiates a cascade of intracellular signaling processes that lead to innate immune cell activation (*8*). This activation is characterized by the induction and secretion of pro-inflammatory cytokines, such as TNF-α and IL-6, as well as enhancement of their phagocytic activity (*9*). Controlled production and secretion of pro-inflammatory cytokines is essential for the development of local inflammation, but in extreme cases, when bacteria reach the bloodstream, uncontrolled activation of phagocytes takes place, resulting in massive secretion of cytokines. These cytokines are mediators in the development of severe sepsis, followed by systemic damage, and in some cases even death (*10*). The role of LPS both in bacterial resistance and in pathogenesis of septic shock emphasizes the importance of improving our understanding of the properties involved in the interactions between LPS and LPS-binding molecules.

[†] This study was supported by the Dr. Josef Cohn Minerva Center for Biomembrane Research. Y.S. is the incumbent of the Harold S. and Harriet B. Brady Professorial Chair in Cancer Research. H.-G.S. acknowledges the German Research Foundation for financial support (Sa 292/10-2).

* To whom correspondence should be addressed: Department of Biological Chemistry, The Weizmann Institute of Science, Rehovot, 76100 Israel. Telephone: 972-8-9342711. Fax: 972-8-9344112. E-mail: Yechiel.Shai@weizmann.ac.il.

[‡] The Weizmann Institute of Science.

[§] University of Bonn.

[1] Abbreviations: AA, amino acid; DDW, double-distilled water; LPS, lipopolysaccharide; AMPs, antimicrobial peptides; LBP, lipopolysaccharide binding protein; TLR, toll like receptor; FTIR, Fourier-transform infrared; CD, circular dichroism; PAMP, pathogen-associated molecular pattern; TNF-α, tumor necrosis factor-α; IL-6, interleukin-6.

10.1021/bi800450f CCC: $40.75
Published on Web 05/23/2008

Table 1: Peptide Designations, Sequences, and HPLC Retention Times

peptide designation	sequence[a]	RP-HPLC retention time (min)[b]
amphipathic-L	L K L L K K L L K K L L K L L-NH_2	38.10
amphipathic-D	L K **L** L K **K** L L **K** K L L **K** L L-NH_2	23.80
scrambled-L	K L K L L K L L K L L K L L K-NH_2	28.05
scrambled-D	K L **K** L L **K** L L **K** L L K **L** L K-NH_2	24.70
segregated-L	L L L L L K K K K K L L L L-NH_2	21.60
segregated-D	L L **L** L L **K** K **K** K K L **L** L L-NH_2	27.66

[a] Underlined and bold amino acids are D-enantiomers. All the peptides are amidated at their C-termini. [b] A C_{18} reverse phase analytical column was used. The peptides were eluted in 60 min, using a linear gradient from 20 to 80% acetonitrile in water, both containing 0.05% TFA (v/v).

Antimicrobial peptides (AMPs) are important components of the innate immune system of all life species (*11*). Several of these peptides can bind LPS and exhibited both antibacterial and LPS detoxification activity (*12–14*). AMPs are produced at the site of infection or inflammation in large quantities and act rapidly to clear the invading microorganism (*15*). These functions are of great interest because of the increasing number of pathogenic bacteria resistant to conventional antibiotics. Therefore, many studies focused on the antibacterial activity of AMPs both in vitro and in vivo (*11, 13*). However, studies on the anti-endotoxic activity of AMPs were reported for only a limited number of native peptides and their derivatives. These peptides neutralize LPS activity both in vitro and in vivo (*14, 16–20*). However, the precise underlying mechanisms and properties of the peptides required for this activity are not yet clear (*21*).

Aiming to achieve this goal, we investigated a series of AMPs and their analogues, all sharing the same amino acid composition (K_6L_9), but their sequences and structures were drastically altered. The list includes all-L-amino acid peptides and their diastereomers (composed of both L- and D-amino acids). Other all L-amino acid peptides composed of K and L have been studied previously for their hemolytic and antimicrobial activities (*22, 23*). Here the peptides were investigated functionally for their antibacterial activity, their ability to block LPS-dependent TNF-α secretion by macrophages, and their ability to bind LPS and affect its oligomeric state. Their secondary structure was characterized in solution, in LPS suspension, and in LPS multibilayers by using CD and FTIR spectroscopy. We discuss our data in light of the findings of the different peptides' properties required for LPS detoxification and for antimicrobial activity.

MATERIALS AND METHODS

Materials. Rink amide MBHA resin and 9-fluorenylmethoxycarbonyl (Fmoc) amino acids were purchased from Calibochem-Novabiochem AG. Other reagents used for peptide synthesis included trifluoroacetic acid (TFA, Sigma), *N*,*N*-diisopropylethylamine (DIEA, Aldrich), methylene chloride (peptide synthesis grade, Biolab), dimethylformamide (peptide synthesis grade, Biolab), and benzotriazolyl-*n*-oxytris(dimethylamino)phosphonium hexafluorophosphate (BOP, Sigma). Dulbecco's modified Eagle's medium (DMEM), heat-inactivated fetal calf serum (FCS), L-glutamine, penicillin−streptomycin amphotericin B antibiotics, and a nonessential amino acid solution (1:100) were supplied by Biological Industries (Beit Haemek, Israel). Bovine serum (BS) was purchased from Hyclone. Lipopolysaccharide from *Escherichia coli* 0111:B4, and fluorescein isothiocyanate (FITC)-conjugated lipopolysccharides were supplied by Sigma.

Peptide Synthesis and Purification. Peptides were synthesized by a solid phase method on rink amide MBHA resin (0.05 mequiv) by using an ABI 433A automatic peptide synthesizer. Labeling of the N-terminus of the peptides with 7-nitrobenz-2-oxa-1,3-diazol-4-yl (NBD) was done on the resin-bound peptide as previously described (*24*). The resin-bound peptides were cleaved from the resins by TFA, washed with dry ether, and extracted with a 30% acetonitrile/water mixture. TFA cleavage of the peptides bound to rink amide MBHA resin resulted in C-terminally amidated peptides. Each crude peptide contained one major peak, as revealed by RP-HPLC, that was 50−70% pure by weight. The peptides were further purified by RP-HPLC on a C_{18} reverse phase Bio-Rad semipreparative column (250 mm × 10 mm, 300 Å pore size, 5 μm particle size). The column was eluted in 40 min, using a linear gradient from 20 to 60% acetonitrile in water, both containing 0.1% TFA (v/v), at a flow rate of 1.8 mL/min. The purified peptides were shown to be homogeneous (>98%) by analytical HPLC. The peptides were further subjected to amino acid analysis and electrospray mass spectroscopy to confirm their composition and molecular weight.

Antibacterial Activity of the Peptides. A set of clinical isolates from distinct patients as well as two standard laboratory strains were included in this study: *Staphylococcus simulans* 22; *Micrococcus luteus* ATCC 1856; *Enterococcus faecium* (I-11054); *Staphylococcus epidermidis*, methicillin-resistant (MRSE; LT1324); *Staphylococcus aureus*, methicillin-susceptible (5185); *S. aureus*, methicillin-resistant (MRSA; LT1338); *Citrobacter freundii* (I-11090); *Klebsiella pneumoniae* (I-10910); *E. coli* (O-19592); *Stenotrophomonas maltophila* (I-10717); *Pseudomonas aeruginosa* (I-10968); and *Candida albicans* (I-11134). In addition, the following control strains were used for activity tests of the peptides: *E. coli* ATCC 12795 and *E. coli* 0111:B4. The strains were maintained on Mueller-Hinton (MH) agar or on blood agar. The determination of the minimal inhibitory concentrations (MICs) of the peptides was performed in microtiter plate assays. Since cationic peptides bind to polystyrene, 96-well polypropylene plates (Life Technologies) were used throughout. A series of 2-fold dilutions in MH broth was prepared from a stock solution of the respective peptide. The indicator strains were grown to an optical density (600 nm) of 1.0 in half-concentrated MH broth and diluted $1:10^5$ with the same medium. Then 100 μL of this suspension was mixed with 100 μL of the peptide dilution in the well of a microtiter plate. After incubation for 18 h (24 h for *M. luteus*) at 37 °C, the MIC was read as the lowest concentration of antimicrobial agent resulting in the complete inhibition of visible growth, and the results are mean values of two independent determinations.

Evaluation of Secretion of TNF-α from RAW264.7 Macrophages. RAW264.7 macrophages were cultured overnight in a 96-well plate (2.5×10^5 cells/well). The medium was then removed followed by the addition to each well of fresh DMEM supplemented with 5% bovine serum. The cells were stimulated with different concentrations of LPS (10, 100, or 1000 ng/mL or 2.5, 25, or 250 nM, respectively) in the

Table 2: Peptide Antibacterial Activities As Reflected in Their Minimal Inhibitory Concentrations (MICs)[a]

peptide	*E. coli* 19592	*E. coli* 0111:B4	*E. coli* ATCC 12795	*P. aeruginosa* I-10968	*St. maltophilia* I-10717	*C. freundii* I-11090	*K. pneumoniae* I-10910
amphipathic-L	12.5	12.5	12.5	12.5	25	25	25
amphipathic-D	0.78	0.78	0.78	1.56	1.56	0.78	1.56
scrambled-L	1.56	3.125	1.56	6.25	3.125	NT	NT
scrambled-D	0.78	0.78	0.78	1.56	6.25	0.78	25
segregated-L	50	50	>50	25	50	>50	>50
segregated-D	0.78	1.56	1.56	3.125	50	3.125	50

peptide	*En. faecium* I-11054	*S. simulans* 22	*S. aureus* 5185	*S. epidermidis*, methicillin-resistant LT1324	*S. aureus*, methicillin-resistant LT1338	*M. luteus* I-11134[b]	*Ca. albicans* ATCC 1856
amphipathic-L	12.5	12.5	12.5	12.5	12.5	6.25	6.25
amphipathic-D	0.78	0.78	0.78	0.39	1.56	0.195	6.25
scrambled-L	NT	NT	NT	NT	3.125	NT	NT
scrambled-D	1.56	0.78	3.125	0.78	6.25	0.39	1.56
segregated-L	12.5	25	>50	50	>50	3.125	3.125
segregated-D	1.56	1.56	12.5	0.78	25	0.39	50

[a] Peptide MICs are in micromolar. [b] MIC determination after 24 h instead of 18 h because of slow growth. NT, not tested.

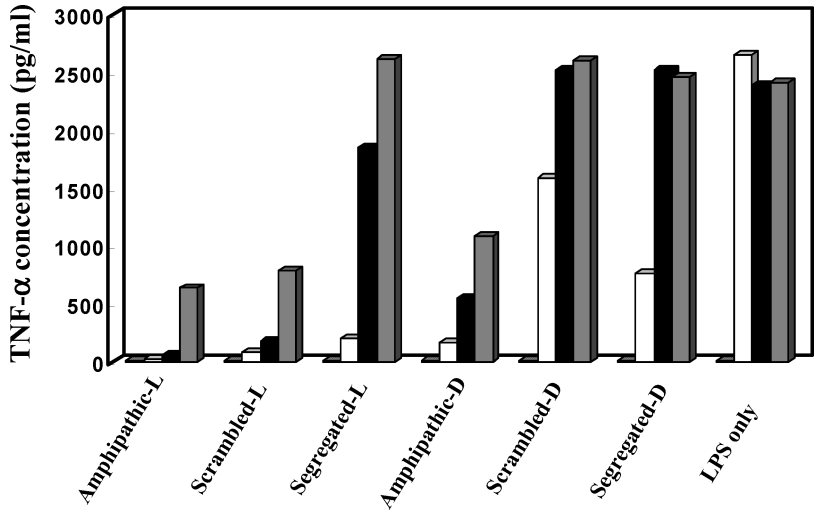

FIGURE 1: Effects of the peptides on LPS-induced TNF-α secretion by macropages. Cells were stimulated with different concentrations of LPS [10 ng/mL (white columns), 100 ng/mL (black columns), and 1000 ng/mL (gray columns)] in the presence or absence of peptides (10 μM). After incubation, the TNF-α concentration in the cell medium was evaluated using a mouse TNF-α ELISA kit. Untreated cells (dotted gray columns) served as controls.

presence 10 μM amphipathic-L, amphipathic-D, scrambled-L, scrambled-D, segregated-L, or segregated-D amino acids. Cells that were stimulated with LPS alone and untreated cells served as controls. The cells were incubated for 6 h at 37 °C followed by collection of samples of the medium from each well. The TNF-α concentration in each of the samples was evaluated using the mouse TNF-α ELISA kit according to the manufacturer's protocol (BIOSOURCE, USA). All experiments were repeated twice.

Binding Assay. The experiments were conducted as described previously (*25*). Briefly, an LPS solution [20 ng/μL (5 μM) in DDW] was added successively to 0.5 μM NBD-labeled peptides (amphipathic-L, scrambled-L, segregated-L, and their diastereomers all dissolved in DDW). The changes in NBD emission (530 nm) were monitored as a function of the LPS:peptide molar ratio using an SLM-AMNICO luminescence spectrometer, with excitation set at 467 nm (8 nm slit) until the system reached equilibrium. To account for background, the emissions of both DDW and LPS alone at the same wavelength were monitored. The changes in the probe emission represented the amount of LPS bound to the peptide because NBD is known to change its emission in a hydrophobic environment (*25*) and, therefore, enable us to evaluate binding of LPS to the peptides. Our system reached binding equilibrium at a certain LPS:peptide ratio. Therefore, the affinity constant could be calculated from the relationship between the equilibrium level of NBD-labeled peptide emission and the LPS concentration, using a steady state affinity model. The affinity constants were, thus, determined by nonlinear least-squares (NLLSQ) fitting using the following equation:

$$Y(x) = K_A X \Delta F_{max} / (1 + K_A X) \quad (1)$$

where X is the LPS concentration, ΔF_{max} is the maximal change in NBD-labeled peptide emission (represents the maximum LPS bound or equilibrium binding response), and K_A is the affinity constant.

Effect of the Peptides on LPS-FITC Aggregates. The assay was conducted as described previously (*14*). Briefly, LPS-FITC (0.5 μg/mL) was treated with increasing concentrations of the peptides. The changes in the emission of FITC (515 nm) were monitored by using an SLM-AMNICO luminescence spectrometer with excitation set at 488 nm (8 nm slit). The emissions of both DDW and peptides alone were taken

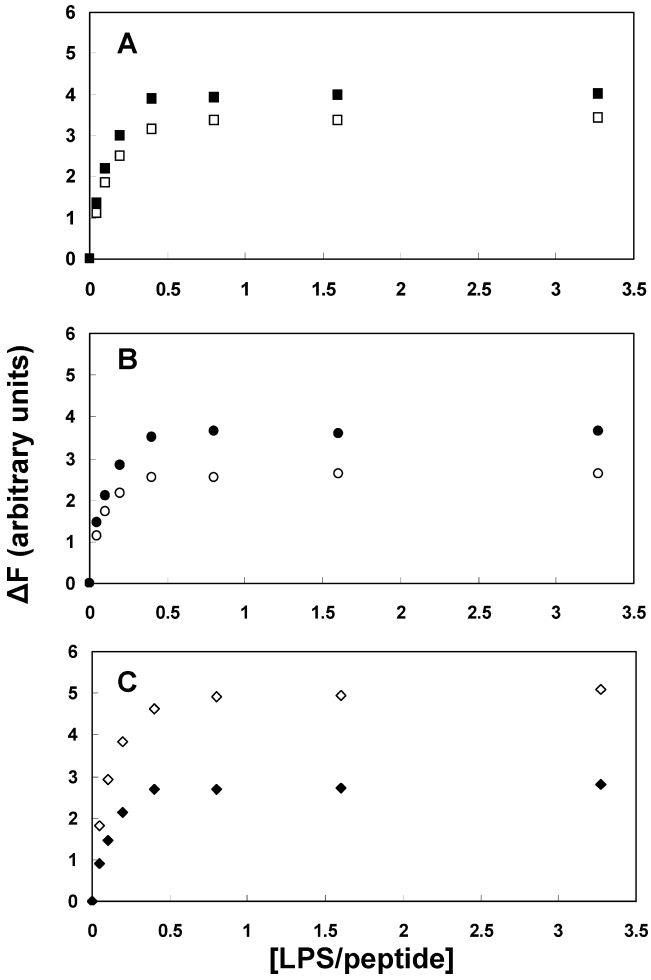

FIGURE 2: Binding of LPS to AMPs. Changes in the fluorescence intensity of the NBD-labeled peptides (ΔF) as a function of the lipid:peptide molar ratio. NBD-labeled peptides (0.5 μM) were titered with LPS. The decrease in NBD emission after addition of LPS relative to the emission of NBD-labeled peptide alone reflects the extent of peptide associated with LPS. Black squares, circles, and triangles represent data for the all-L-amino acid peptides; white symbols represent data for the D,L-peptides. The results are the means of three independent experiments with a standard deviation of ±10%.

as a background. Dissociation of the aggregates results in an increase in the fluorescence of FITC due to dequenching (*26*). We followed the changes in FITC emission until the system reached a steady state.

Electron Microscopy. We used transmission electron microscopy (TEM) to visualize the effect of the peptides on LPS aggregates. An LPS suspension in PBS (1 mg/mL) was incubated for 1 h with 20 or 50 μM amphipathic-L (an effective LPS neutralizer) or with the same concentration of scrambled-D (weak LPS neutralizer). A drop from each treatment was deposited onto a carbon-coated grid and negatively stained with uranyl acetate (1%). The grids were examined using a JEOL JEM 100B electron microscope (Japan Electron Optics Laboratory Co., Tokyo, Japan), at 60 kV, with a magnification of 30000×. Untreated LPS was used as a control.

Fourier-Transform Infrared (FTIR) Spectroscopy Measurements. This technique was used to obtain information about the influence of LPS on the secondary structure of the peptides. Spectra were obtained with a Bruker equinox 55 FTIR spectrometer equipped with a deuterated triglyceride sulfate (DTGS) detector and coupled to an ATR device as previously described (*27*). Briefly, a mixture of LPS (1 mg) alone or with a peptide (~80 μg) (LPS to peptide molar ratio of ~5:1) was deposited on a ZnSe horizontal ATR prism (80 mm × 7 mm). Lipid/peptide mixtures were prepared by dissolving them together in a 1:2 MeOH/CH_2Cl_2 mixture and drying under a stream of dry nitrogen while moving a Teflon bar back and forth along the ZnSe prism. Spectra were recorded, and the respective pure phospholipid spectra were subtracted to yield the difference spectra. The background for each spectrum was a clean ZnSe prism. Hydration of the sample was achieved via introduction of excess deuterium oxide ($2H_2O$) into a chamber placed on top of the ZnSe prism in the ATR casting and incubation for 15 min before acquisition of the spectra. H−D exchange was considered complete after the total shift of the amide II band. Any contribution of $2H_2O$ vapor to the absorbance spectra near the amide I peak region was eliminated by subtracting the spectra of pure lipids equilibrated with $2H_2O$ under the same conditions.

ATR-FTIR Data Analysis. Prior to curve fitting, a straight baseline passing through the cordinates at 1700 and 1600 cm^{-1} was subtracted. To resolve overlapping bands, the spectra were processed using PEAKFITTM (Jandel Scientific, San Rafael, CA). Second-derivative spectra were calculated to identify the positions of the component bands in the spectra. These wavenumbers were used as initial parameters for curve fitting with Gaussian component peaks. Position, bandwidths, and amplitudes of the peaks were varied until (i) the resulting bands shifted by no more than 2 cm^{-1} from the initial parameters, (ii) all the peaks had reasonable half-widths (<20−25 cm^{-1}), and (iii) good agreement between the calculated sum of all the components and the experimental spectra was achieved ($r^2 > 0.99$). The relative contents of the different secondary structure elements were estimated by dividing the areas of individual peaks, assigned to a specific secondary structure, by the whole area of the resulting amide I band. The results of two independent experiments were averaged.

The interactions of the peptides with LPS headgroups were studied by monitoring the symmetric stretching vibration of the negatively charged phosphate groups, $\upsilon_s(PO_2^-)$, ranging from 1200 to 1280 cm^{-1} (*28*).

Circular Dichroism (CD) Spectroscopy. The CD spectra of the peptides were measured with a Jasco J-500A spectropolarimeter after the instrument had been calibrated with (+)-10-camphorsulfonic acid. The spectra were scanned at 25 °C in a capped, quartz optical cell with a path length of 0.5 mm. Spectra were obtained at wavelengths of 250−190 nm. Eight scans were taken for each peptide at a scan rate of 20 nm/min. Mean residue ellipticities were expressed as [θ] (degrees square centimeters per decimole). The peptides (25 μM) were scanned in the presence or absence of LPS (25 μM) dissolved in PBS. Fractional helicity was calculated from the dichroic minimum at 222 nm, as previously described (*29, 30*). The $\theta_{222}/\theta_{208}$ ratio was calculated to estimate helix−helix interactions (*31*).

RESULTS

Peptide Synthesis, Purification, and Antimicrobial Activity. Six cationic peptides were synthesized and investigated. The parental 15-mer peptide (K_6L_9) was designed to fold into an

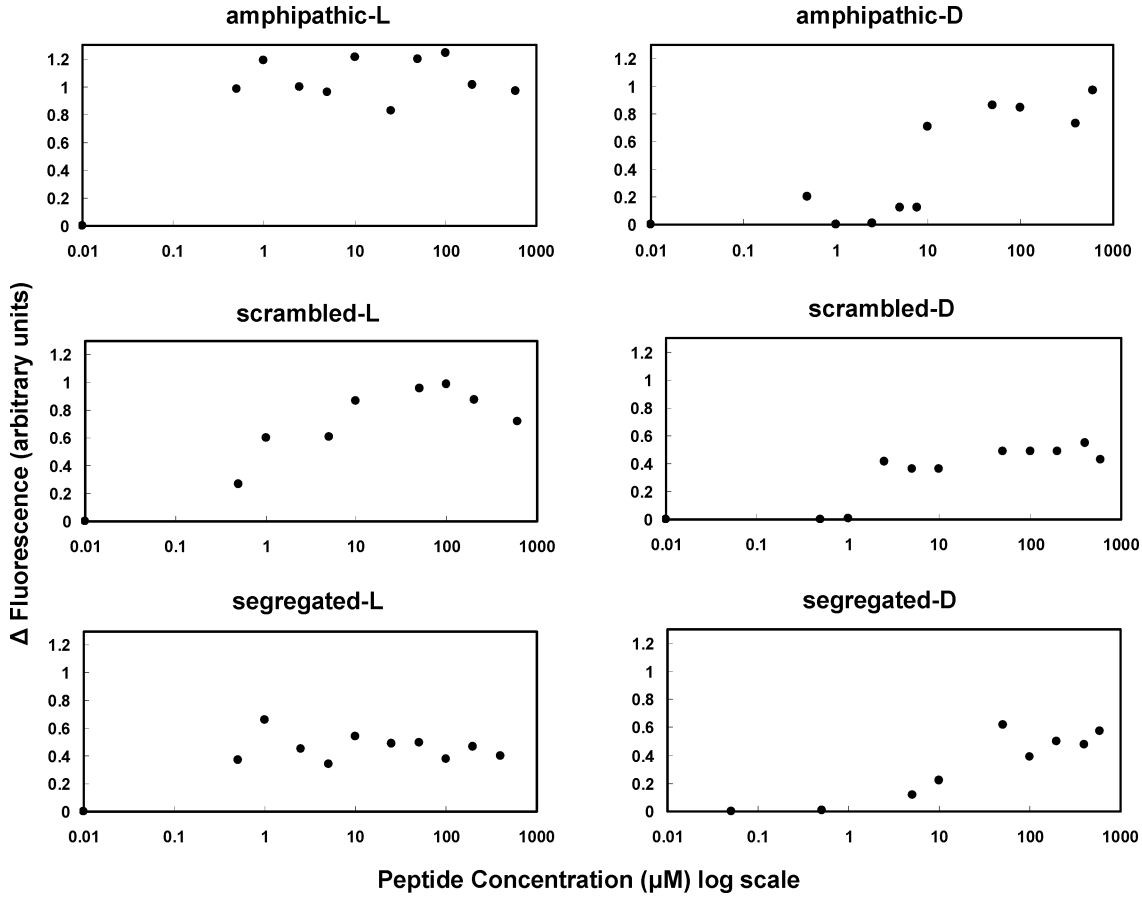

FIGURE 3: Relationship between peptide concentration and the LPS-FITC aggregation state. LPS-FITC (0.5 μg/mL) was treated with decreasing concentrations of peptides. The change in FITC emission after each treatment was monitored until it reached equilibrium. The emission increase reflected the change in the LPS-FITC aggregate state. FITC tends to increase its emission when the distance between its monomers increases.

Table 3: Calculated Affinity Constants of the Different Peptides for LPS in Suspension[a]

peptide	affinity constant (M^{-1})	R^2
amphipathic-L	$(2.19 \pm 3.0) \times 10^7$	0.98
amphipathic-D	$(2.09 \pm 0.22) \times 10^7$	0.99
scrambled-L	$(2.56 \pm 0.31) \times 10^7$	0.99
scrambled-D	$(3.20 \pm 0.33) \times 10^7$	0.99
segregated-L	$(2.12 \pm 0.32) \times 10^7$	0.98
segregated-D	$(2.39 \pm 0.19) \times 10^7$	0.99

[a] The affinity constants were determined by nonlinear least-squares (NLLSQ) fitting.

ideal amphipathic α-helix in its all-L-amino acid form. The second peptide had a scrambled sequence of hydrophobic and positively charged amino acids, and in the third one, we segregated the hydrophobic and positively charged amino acids. The other three peptides were the corresponding diastereomers of the mentioned peptides (see Table 1). Note that all the peptides share the same amino acid composition. However, the HPLC retention time was different, indicating that sequence alteration affected the peptides' effective hydrophobicity. In general, the incorporation of D-amino acids into the sequence of the peptides caused a reduction in their retention time, indicating that their effective hydrophobicity is lower. Interestingly, the opposite trend was observed with the segregated peptides in which the retention time of the all-L-peptide is shorter than that of the D-peptide. Note that the segregated-L peptide adopts mainly an aggregated β-sheet structure in solution and when bound to hydrophobic surfaces (LPS). Such large aggregates could elute earlier than expected for less aggregated forms. The antimicrobial activity of the peptides was tested against 13 different strains of Gram-negative and Gram-positive bacteria and one fungal strain, among them nine clinically isolated strains that are multiresistant to conventional antibiotics. The data reveal that all the peptides, despite their drastic sequence alterations, are antimicrobial, most of which are of very high potency. Interestingly, the overall trend is that the D,L-amino acid analogues are significantly more active than their all-L-amino acid parental peptides (Table 2).

Effect of the Peptides on LPS-Induced Secretion of TNF-α by RAW264.7 Macrophages. TNF-α is one of the first pro-inflammatory cytokines secreted by LPS-stimulated immune cells (*9*). To explore the effect of the peptides on LPS-induced TNF-α secretion, we first stimulated macrophages with LPS at three concentrations, 10, 100, and 1000 ng/mL (2.5, 25, and 250 nM, respectively). The ability of the peptides to detoxify LPS was examined by monitoring the concentration of the secreted TNF-α in the presence of the peptides (10 μM). The data shown in Figure 1 reveal that all the peptides reduced the level of TNF-α secretion when the macrophages were stimulated with 10 ng/mL (2.5 nM) LPS [LPS concentration that is similar to that found in septic patients (*32*)]. Note that scrambled-D and segregated-D were significantly less active compared with the others, which reduced TNF-α almost to the basal level. However, when macrophages were stimulated with LPS at higher concentra-

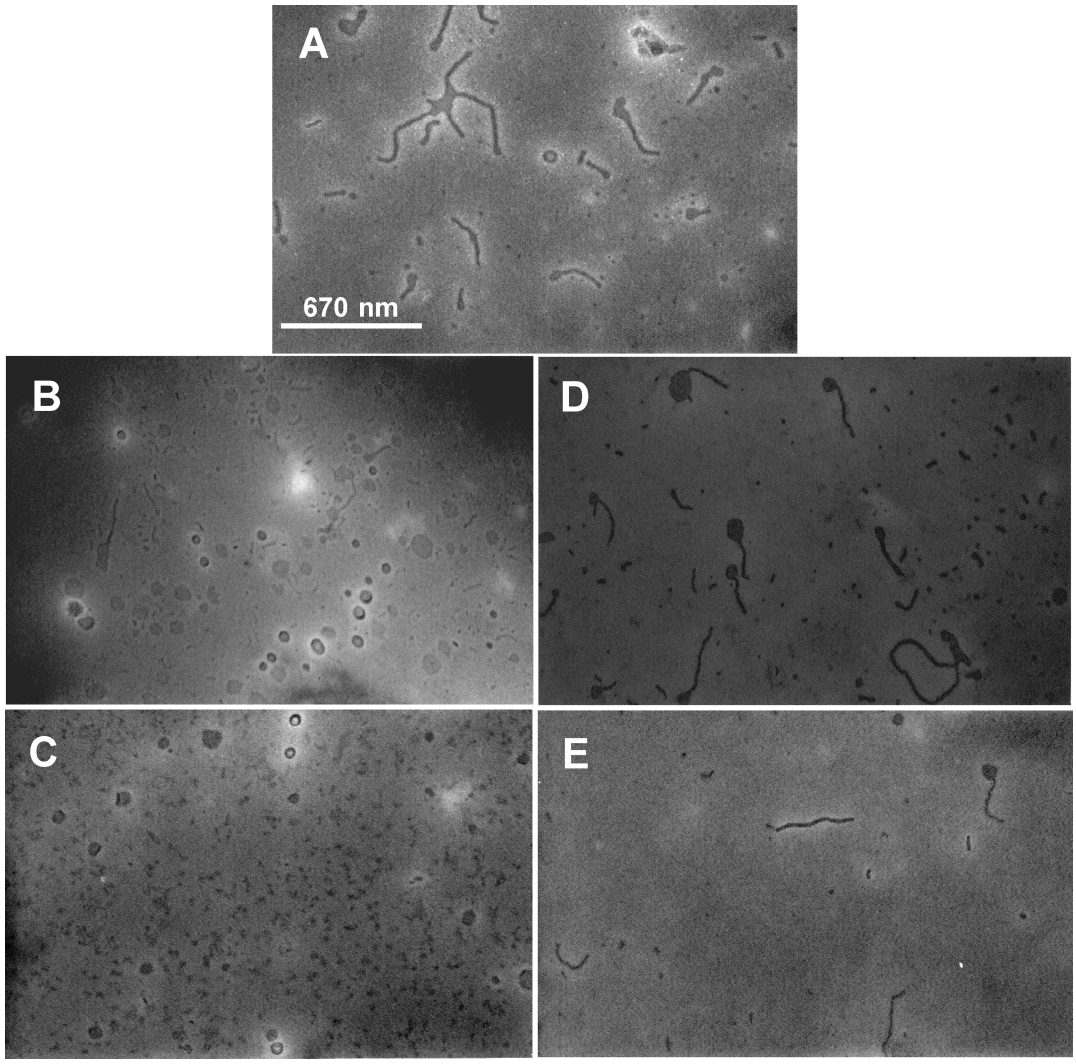

FIGURE 4: Electron micrographs of a negatively stained LPS suspension. (A) Untreated LPS. (B and C) LPS treated with 20 and 50 μM amphipathic-L, respectively. (D and E) LPS treated with 20 and 50 μM scrambled-D, respectively. All samples were negatively stained with uranyl acetate (1%).

tions [100 and 1000 ng/mL (25 and 250 nM, respectively)], only amphipathic-L, amphipathic-D, and scrambled-L significantly reduced the TNF-α concentrations. As we will discuss later, the most active peptides either adopted an α-helical structure or had an amphipathic character both in the all-L or the D,L forms.

Binding of the Peptides to LPS. The ability of antimicrobial peptides to bind LPS is a prerequisite for their antibacterial and endotoxin detoxifying activities. We conducted binding experiments by using NBD-labeled peptides as described previously (*25, 33*). Changes in the intensities of the fluorescence emission of the NBD-labeled peptides (*F*) were recorded as a function of the LPS:peptide molar ratios and are shown in Figure 3. The data were fitted by using NLLSQ fitting to determine the binding constants (K_a). We found that all the peptides bound with high and similar affinities to LPS ($K_a = 10^7$ M^{-1}) (Table 3), despite the differences in their antibacterial and LPS neutralizing activities.

Effect of the Peptides on LPS-FITC Aggregates. We have shown previously a direct correlation between the ability of amphipathic α-helical AMPs to disaggregate LPS oligomers and their ability to neutralize LPS (*14*). Here we tested the ability of all the peptides to disaggregate LPS to determine whether this is a general property of LPS-neutralizing agents irrespective of their structure. This was done by monitoring the changes in the fluorescence of LPS-FITC, which is dequenched in the aggregated form but increases once the aggregates dissociate (*26*). Results are shown in Figure 3. The data revealed two major groups. The first includes the most active peptides, namely, amphipathic-L, amphipathic-D, and scrambled-L, all of which exhibited a strong ability to dissociate LPS aggregates. The second group includes scrambled-D, segregated-L, and segregated-D, which were less active in this assay. These results are in agreement with the ability of the peptides to detoxify LPS, as reflected in the reduced level of TNF-α secretion by macrophages (Figure 1). Note that although all the peptides became active above a threshold concentration ("all or none effect"), this concentration was significantly lower (~1 μM) for the all-L-amino acid peptides, compared with their diastereomeric counterparts (>5 μM). This occurs despite the finding that they all bind to LPS with a stoichiometry of ~1:1 (Figure 2).

Visualizing the Effect of the Peptides on LPS Aggregates. TEM was used to visualize the effect of the peptides on LPS aggregates. On the basis of the results of LPS neutralization and LPS-FITC disaggregation, we have focused on two peptides: the active amphipathic-L and the nonactive scram-

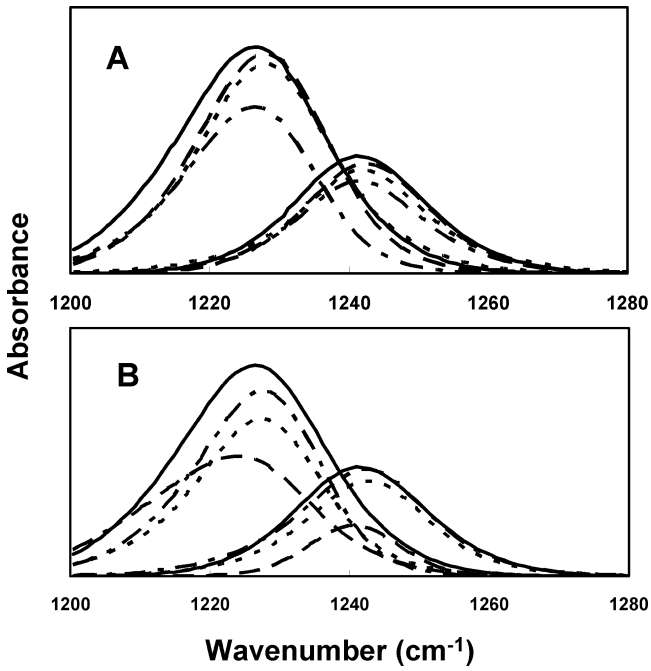

FIGURE 5: Influence of the different peptides on the headgroups of LPS. IR absorbance spectra are shown for LPS multibilayers in the range of the antisymmetric stretching vibration of the negatively charged phosphates, $\upsilon_{as}(PO_2^-)$, for the different peptides: (A) all-L-amino acid peptides and (B) D,L-amino acid peptides. Designations are as follows: LPS (—), scrambled (—•—), segragated (•••), amphipathic (———).

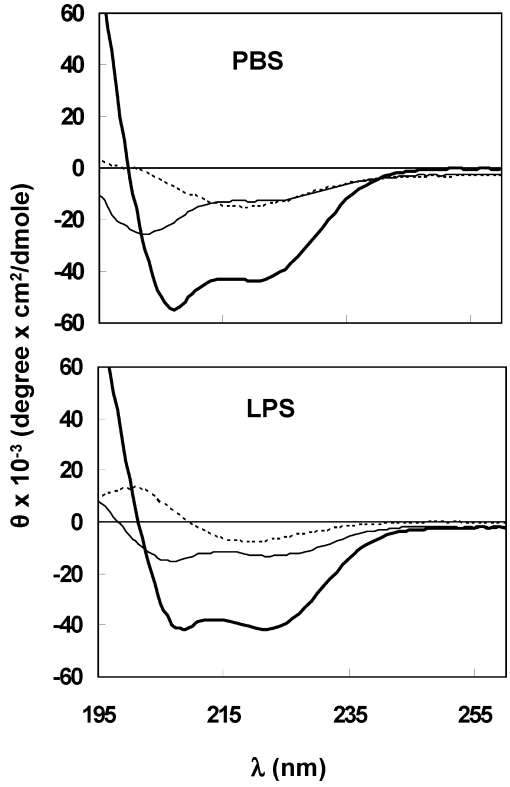

FIGURE 6: CD spectra of the peptide. Spectra were recorded after 25 μM peptide was dissolved in LPS suspension (25 μM) or in PBS: (thick line) amphipathic-L, (thin line) scrambled-L, and (dashed line) segregated-L.

bled-D. LPS in suspensions formed fiberlike aggregates (Figure 4). These aggregates were completely broken into smaller particles by amphipathic-L when used at its high active concentration (Figure 4C). However, scrambled-D, although it reduced the number of LPS aggregates at the high concentration (50 μM), had almost no effect on the number of aggregates and structure when applied at a lower concentration (20 μM). This observation supports the results of LPS-FITC disaggregation (Figure 3), suggesting that the mechanism of LPS neutralization by these peptides involves strong binding to LPS followed by breaking LPS aggregates to smaller particles that are not available to LBP.

Interaction of the Peptides with the LPS Phosphate Groups. The interaction of the peptides with the LPS phosphate groups is a way of estimating the depth of the penetration of the peptides into the LPS layer. This can reflect the potential of the peptide to traverse the outer membrane of the bacteria (*34, 35*). We followed the antisymmetric stretching vibration of the negatively charged phosphate, $\upsilon_{as}(PO_2^-)$ (1200−1300 cm^{-1}). In the range of this vibration, namely, 1220 and 1240 cm^{-1}, a drastic change in the band shape is seen as a result of such an interaction (*28*). The addition of the peptides led to a reduction in the band intensities, indicating intercalation of the peptide closer to the lipid A phosphate groups. Interestingly, the binding of the diastereomers to LPS led to similar significant reductions in the band intensity, with the strongest effect induced by amphipathic-D (Figure 5). These results correlate with the highest antibacterial activity of all the diastereomers compared with their all L-amino acid counterparts. In contrast, large differences were found between the all-L-amino acid peptides. Interestingly, however, the strongest effect was observed with scrambled-L, which has significantly higher antimicrobial activity than the other two L-amino acid peptides. Note, however, that there is no correlation between LPS neutralizing activity and the intercalation of the peptides near the phosphate groups, since, for example, amphipathic-D has the strongest effect on the phosphates whereas amphipathic-L has the weakest effect. Yet both are highly potent in neutralizing the LPS toxic effect (Figure 1). This is probably due to the differences in the peptides' structures and oligomeric state, which affect their ability to reach the less exposed inner phosphate group (see below).

Secondary Structure of the Peptides in Solution and in LPS Suspension Determined by CD Spectroscopy. The secondary structures of the all-L-amino acid peptides (at 25 μM) were determined in LPS suspension (25 μM) and in PBS (Figure 6). The diastereomers did not give any detectable signal due to the incorporation of the D-amino acids and therefore are not shown. The data revealed an 100% α-helical structure for amphipathic-L, both in PBS and in LPS suspension, characterized by double minima at 208 and 222 nm. Scrambled-L seems to adopt a low level of helical structure and random coil in PBS but adopted a 37% α-helical structure in LPS suspension, whereas segregated-L exhibited a single minimum at 215 nm, both in PBS and in LPS suspension, typical of a β-sheet structure. None of the D,L-peptides gave any signal in PBS or in LPS suspension. A defined α-helical structure of amphipathic-L or β-sheet of segregated-L in PBS indicates that the peptide probably forms oligomers. This is because a short peptide can form a distinct secondary structure in solution when it oligomerizes. In the oligomeric form, the hydrophobic surfaces are packed one against another and the hydrophilic surfaces face the solution (*36, 37*). As we will show next, the CD structures in LPS agree with those obtained using FTIR spectroscopy.

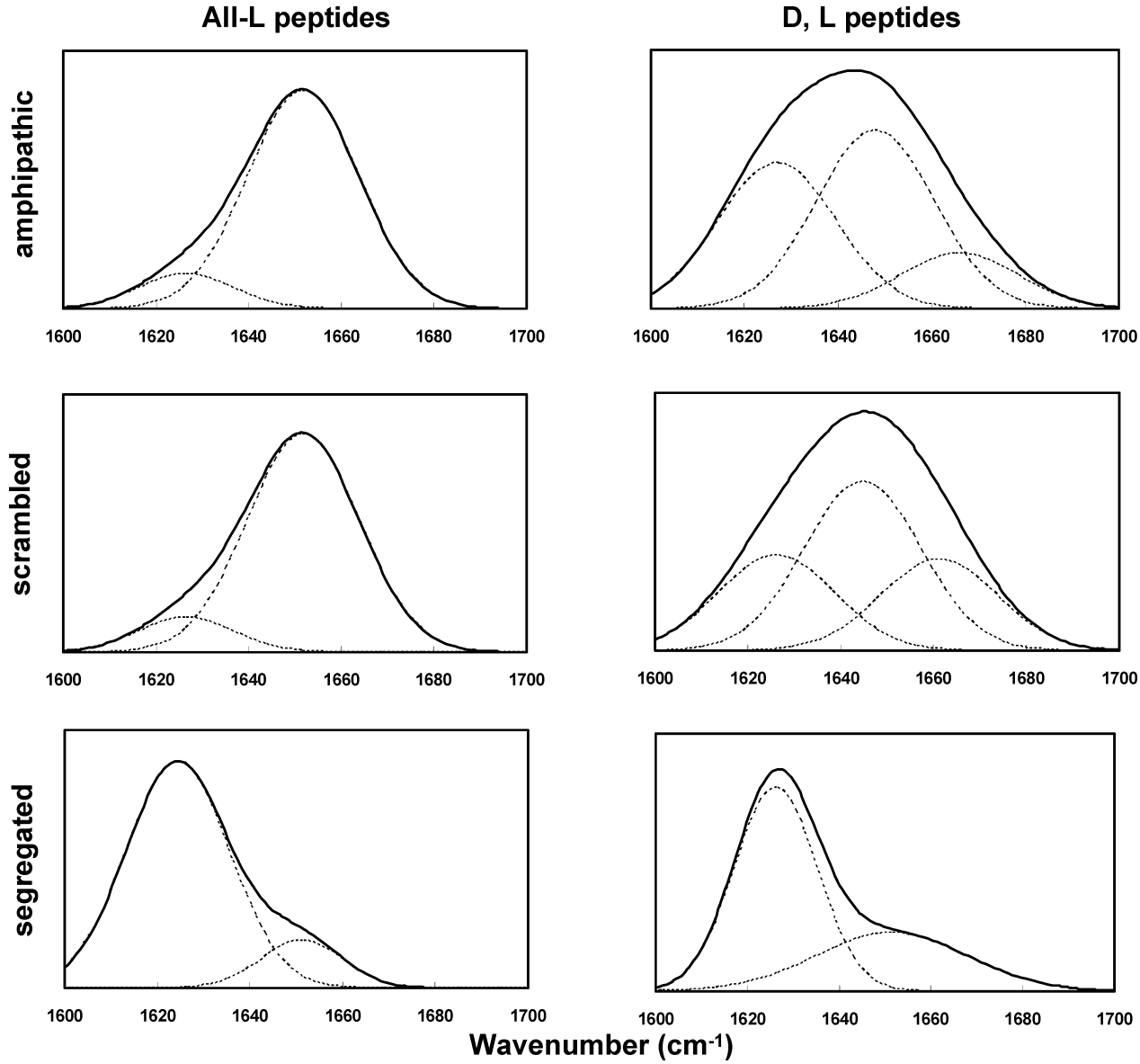

FIGURE 7: Deconvolution of FTIR spectra of the fully deuterated amide I band (1600−1700 cm^{-1}) of peptides in LPS multibilayers. Second derivatives were calculated to identify the positions of the component bands in the spectra. The component peaks result from curve fitting using a Gaussian line shape. The sums of the fitted components superimpose on the experimental amide I region spectra. Solid lines represent the experimental FTIR spectra; broken lines represent the fitted components.

Table 4: Peptide Structure As Determined by ATR-FTIR Spectroscopy from the Deconvolution of the Amide I Bands of the All-L and the Diastereomeric Peptides Incorporated into LPS Multibilayers[a]

peptide designation	β-sheet + aggregated strands (%), 1620−1640 cm^{-1}	random coil/ α-helix (%), 1640−1654 cm^{-1}	distorted/ 3_{10}-helix (%), 1655−1670 cm^{-1}
amphipathic-L	10	90	−
amphipathic-D	38	47	15
scrambled-L	10	90	−
scrambled-D	25	50	25
segregated-L	85	15	−
segregated-D	65	35	−

[a] A 10:1 lipid:peptide molar ratio was used.

Secondary Structure of the Peptides in LPS Multibilayers, As Determined by Spectroscopy. The secondary structure components of the peptides were determined from the wavenumbers of the amine I vibration (followed by deconvolution) after complete deuteration. The amide I region spectra as well as the fitted band components (obtained by deconvolution) of the peptides when bound to LPS multibilayers are shown in Figure 7. Assignment of the different secondary structures to the various amide I regions was conducted according to the values taken from other work (*38, 39*) and from our previous results (*40, 41*). The assignments and the relative areas of the component peaks are summarized in Table 4. The results indicate strong bands typical of α-helical structures at 1650 cm^{-1} (90%) and a small portion of aggregated β-sheet at 1625 cm^{-1} (10%), for both amphipathic-L and scrambled-L. Note that amphipathic-D and scrambled-D adopted similar structures with bands typical of α-helical structures at 1650 cm^{-1}, 3_{10}-helix at 1658 cm^{-1}, and aggregated β-sheet at 1625 cm^{-1}. In comparison, segregated-L and segregated-D adopted mainly an aggregated β-sheet structure (85 and 65%, respectively), and only a small portion of an α-helical structure. Similar structures were reported previously for these peptides in a PE/PG model membrane (*42*).

Table 5: Summary of All the Biophysical Properties of the Peptides

peptide	antimicrobial activity	LPS detoxification	peptide structure: LPS	peptide structure: PE/PG inner membrane[a]	LPS disaggregation	effect on phosphate group	binding to LPS
amphipathic-L	+	+++	α-helix	α-helix	+++	+	+++
amphipathic-D	+++	+++	α-helix/distorted helix	α-helix/distorted helix	+++	+++	+++
scrambled-L	+++	+++	α-helix	β-sheet	+++	+++	+++
scrambled-D	+++	±	α-helix/distorted helix	α-helix/distorted helix	+	+++	+++
segregated-L	±	++	β-sheet	β-sheet	++	+	+++
segregated-D	+++	+	β-sheet/α-helix	β-sheet/α-helix/distorted helix	+	+++	+++

[a] Taken from ref *42*.

DISCUSSION

The important conclusion from our study is that the overall biophysical properties of the cationic antimicrobial peptides studied here needed to kill bacteria are not the same as those needed to detoxify LPS, and that we identified specific biophysical properties of the peptides that are required for each function. These properties include sequence, an amphipathic structure, affinity for LPS, the ability to traverse the LPS layer, and the ability to disaggregate LPS micelles. These findings can be achieved by using a group of peptides that all share the same amino acid composition but with sequences drastically altered. Since all the peptides bound similarly to LPS (Figure 2 and Table 3), we can assume that the differences in their activities are not due to differences in the amount of bound peptide but instead are due to other properties of the peptides. Note that we used LPS, which is derived from one of the bacterial strains listed in Table 2 (0111:B4).

Effect of Primary Sequence Alteration on the Biophysical Properties and the Antimicrobial Potency of the Peptides. Alteration of the primary sequence of the peptides only partially affected their antimicrobial activity against the tested bacteria that also include clinically resistant strains (Table 2). In fact, besides segregated-L, all other drastically altered peptides improved their antimicrobial activity, compared with the parental molecule amphipathic-L. It has been suggested that bacteria can resist a specific antibacterial peptide by preventing it from traversing LPS, the external barrier of the bacteria (*35, 43*). This property is reflected by the potential of the peptide to decrease the magnitude of the signal of the antisymmetric stretching vibrations of the negatively charged phosphate $\upsilon_{as}(PO_2^-)$ of LPS, located close to the lipid hydrophobic anchor, lipid A (*34, 35*). The results of the ATR-FTIR studies (Figure 5) support this hypothesis, since sequence alteration improved the ability of the peptides to penetrate more deeply, closer to lipid A. Thus, the most potent antimicrobial peptides, namely, amphipathic-D, scrambled-D, segregated-D, and scrambled-L, had the strongest effect on the phosphate groups. An interesting observation is that in all cases the activities of the D,L-peptides are better than those of their all-L-forms, which is probably due to the structural alteration of the D,L-peptides compared with the L-peptides rather than the ability of the D,L-peptides to resist enzymatic degradation. In support of this, our results show a direct correlation between the antibacterial activity and the disruptive effects of the peptides on the LPS and/or the inner phospholipid bilayer. For example, the all-L-scrambled peptide is as potent as its D,L-counterpart, yet it is not resistant to enzymatic degradation. Nevertheless, we have already shown that D,L-containing peptides are more resistant to proteolysis (*42*). Therefore, we cannot rule out some contribution from their partial resistance to degradation to their activity. An interesting question is why the less structured peptides can better traverse the LPS despite the finding that all of them bind similarly to LPS (Figure 2 and Table 3). Our data indicate that the answer could lie in the differences in the structure of the peptides in solution. CD spectroscopy results (Figure 6) showed that amphipathic-L has a predominant α-helical structure in solution, segregated-L adopted a β-strand structure, whereas scrambled-L did not adopt a defined structure. The D,L-peptides did not show any significant results, partly because of the incorporation of the D-amino acids within the sequences. A short peptide can have a defined structure in solution, as a consequence of oligomerization of the peptides, such that the hydrophobic surfaces are packed one against another and the hydrophilic surfaces face the solution (*37*). It is therefore difficult for such oligomers to traverse the LPS barrier, whereas it is much easier for the peptides's monomers to penetrate. In support of this explanation, the two structured peptides, amphipathic-L and segregated-L, are the least potent. In addition, the better flexibility of the D,L-peptides could allow them to take the preferred membrane-active structure once they are bound to the membrane, much easier than the more rigid and aggregated all-L-amino acid peptides. Sequence alteration modified the amphipathic property that typifies most cationic antimicrobial peptides (*44, 45*). This property is important for the initial binding of the peptide to the bacteria's negatively charged outer surface and for the ability of the peptide to perturb the membrane (*46*).

ATR-FTIR revealed that binding of the peptides to LPS stabilizes their structure within the membrane (Table 3 and Figure 7), which is similar with what has been found with other AMPs when bound to negatively charged phopholipid vesicles such as PC/PS or PE/PG membranes (*34, 47, 48*). The structures of the peptides can be classified into three different groups: (i) α-helices (amphipathic-L and scrambled-L), (ii) distorted helix (amphipathic-D and scrambled-D), and (iii) β-sheet (segregated-L and segregated-D). Table 2 reveals that there is no structural requirement once there is an appropriate balance between the number of hydrophobic amino acids and positively charged amino acids.

Effect of Primary Sequence Alteration on the Capability of the Peptides To Detoxify LPS. Several AMPs could bind LPS in suspension and block its endotoxic effects both in vitro and in vivo (*16–20*). However, practically all AMPs tested so far for this activity adopt an amphipathic α-helix upon their binding to membranes. Here we compared the LPS neutralizing activity of an amphipathic α-helix (am-

phipathic-L) with that of its structurally altered analogues to determine whether a specific amphipathic structure is indeed required, and whether there is a direct correlation between LPS neutralizing and antimicrobial activities. The data reveal two interesting findings. (i) In contrast with the antimicrobial activity, potent LPS neutralizing activity, as reflected in the amount of TNF-α secreted by the macrophages in the presence of LPS at all concentrations, requires a well-defined helical structure (amphipathic-L, scrambled-L, and amphipathic-D) (Figure 1). (ii) However, when the macrophages were stimulated with a low concentration of LPS [10 ng/mL (2.5 nM)], the other peptides also exhibited activity. In that case, segregated-L was highly potent. Note that this peptide adopts a predominatly β-sheet structure. To the best of our knowledge, this is the first example of a linear β-sheet peptide that is highly potent in detoxifying LPS.

Binding to LPS is the initial step for both antibacterial activity and LPS neutralization by the peptides. As mentioned before, all peptides have similar affinities for LPS, and therefore, other characteristics of the peptides should affect their ability to neutralize LPS. Previously, we have shown that the peptides' ability to neutralize LPS correlates with their ability to adopt an amphipathic α-helical structure and to disaggregate LPS in suspension (*14*). LPS has previously been shown to form fiberlike aggregates (*49, 50*). Here we used this assay and examined whether the peptides need a specific structure to have LPS neutralizing activity. Importantly, we found that all the active peptides strongly bind LPS to form LPS−peptide complexes that are smaller than LPS aggregates alone (Figures 3 and 4). These particles probably reduce the availability of LPS to bind LBP, resulting in a decrease in the level of TNF-α secretion by macrophages. This activity of the peptides does not depend on their specific structure, since the α-helical amphipathic-L, the unstructured scrambled-L, and the β-sheet segregated-L all can neutralize LPS. Note that other investigators have shown that some linear and cyclic AMPs cause an increase in LPS aggregate diameter, suggesting that these peptides interact with LPS to form large multilammelar stacks (*51–53*). Note, however, that the LPS used in these studies was derived from mutated bacteria that lack some of the saccharidic portion of LPS, which might explain the differences between our results and others.

A summary of the activities and biophysical properties of the peptides is given in Table 5. The data indicate several biophysical properties that are required for potent antimicrobial activity compared to those required for potent LPS neutralizing activity. (i) Peptides with only potent LPS neutralizing activity are characterized by having a stabilized structure in both the outer LPS membrane and the inner PE/PG membrane (either α-helical or β-sheet). Furthermore, they have a weak effect on the LPS phosphate groups and are potent in disaggregating LPS micelles. (ii) Peptides with only potent antimicrobial activity have unstable structures in both LPS and PE/PG membranes and have a strong effect on the LPS phosphate groups. (iii) Peptides with both antimicrobial and LPS neutralizing activities have defined and flexible structures, can disintegrate LPS micelles, and have a strong effect on the LPS phosphate groups.

Besides shedding light on the peptides' parameters that are involved in antimicrobial and LPS detoxifying activities, this study should assist in the development of host-defense mimicking peptides that carry one function or both antimicrobial and LPS neutralizing activities. Such peptides are urgently needed due to the increasing resistance of bacteria to available antibiotics.

ACKNOWLEDGMENT

We thank Monika Eschbach-Bludau for expert technical help and to Dr. Yehuda Marikovsky for technical support in the transmission electron microscopy studies.

REFERENCES

1. Nikaido, H. (1994) Prevention of drug access to bacterial targets: Permeability barriers and active efflux. *Science 264*, 382–388.
2. Snyder, D. S., and McIntosh, T. J. (2000) The lipopolysaccharide barrier: Correlation of antibiotic susceptibility with antibiotic permeability and fluorescent probe binding kinetics. *Biochemistry 39*, 11777–11787.
3. Nikaido, H., and Vaara, M. (1985) Molecular basis of bacterial outer membrane permeability. *Microbiol. Rev. 49*, 1–32.
4. Hancock, R. E. (1984) Alterations in outer membrane permeability. *Annu. Rev. Microbiol. 38*, 237–264.
5. Ginsburg, I. (2002) The role of bacteriolysis in the pathophysiology of inflammation, infection and post-infectious sequelae. *APMIS 110*, 753–770.
6. Ulevitch, R. J., and Tobias, P. S. (1999) Recognition of gram-negative bacteria and endotoxin by the innate immune system. *Curr. Opin. Immunol. 11*, 19–22.
7. Tobias, P. S., Soldau, K., and Ulevitch, R. J. (1986) Isolation of a lipopolysaccharide-binding acute phase reactant from rabbit serum. *J. Exp. Med. 164*, 777–793.
8. Poltorak, A., He, X., Smirnova, I., Liu, M. Y., VanHuffel, C., Du, X., Birdwell, D., Alejos, E., Silva, M., Galanos, C., Freudenberg, M., Ricciardi-Castagnoli, P., Layton, B., and Beutler, B. (1998) Defective LPS signaling in C3H/HeJ and C57BL/10ScCr mice: Mutations in Tlr4 gene. *Science 282*, 2085–2088.
9. Zhang, F. X., Kirschning, C. J., Mancinelli, R., Xu, X. P., Jin, Y., Faure, E., Mantovani, A., Rothe, M., Muzio, M., and Arditi, M. (1999) Bacterial lipopolysaccharide activates nuclear factor-κB through interleukin-1 signaling mediators in cultured human dermal endothelial cells and mononuclear phagocytes. *J. Biol. Chem. 274*, 7611–7614.
10. Cohen, J. (2002) The immunopathogenesis of sepsis. *Nature 420*, 885–891.
11. Boman, H. G. (1995) Peptide antibiotics and their role in innate immunity. *Annu. Rev. Immunol. 13*, 61–92.
12. Jerala, R., and Porro, M. (2004) Endotoxin neutralizing peptides. *Curr. Top. Med. Chem. 4*, 1173–1184.
13. Hancock, R. E., and Scott, M. G. (2000) The role of antimicrobial peptides in animal defenses. *Proc. Natl. Acad. Sci. U.S.A. 97*, 8856–8861.
14. Rosenfeld, Y., Papo, N., and Shai, Y. (2006) Endotoxin (Lipopolysaccharide) Neutralization by Innate Immunity Host-Defense Peptides: Peptide Properties and Plausible Modes of Action. *J. Biol. Chem. 281*, 1636–1643.
15. Zasloff, M. (2002) Antimicrobial peptides of multicellular organisms. *Nature 415*, 389–395.
16. Scott, M. G., Rosenberger, C. M., Gold, M. R., Finlay, B. B., and Hancock, R. E. (2000) An α-helical cationic antimicrobial peptide selectively modulates macrophage responses to lipopolysaccharide and directly alters macrophage gene expression. *J. Immunol. 165*, 3358–3365.
17. Andra, J., Koch, M. H., Bartels, R., and Brandenburg, K. (2004) Biophysical characterization of endotoxin inactivation by NK-2, an antimicrobial peptide derived from mammalian NK-lysin. *Antimicrob. Agents Chemother. 48*, 1593–1599.
18. Motobu, M., Amer, S., Yamada, M., Nakamura, K., Saido-Sakanaka, H., Asaoka, A., Yamakawa, M., and Hirota, Y. (2004) Effects of antimicrobial peptides derived from the beetle *Allomyrina dichotoma* defensin on mouse peritoneal macrophages stimulated with lipopolysaccharide. *J. Vet. Med. Sci. 66*, 319–322.
19. Larrick, J. W., Hirata, M., Balint, R. F., Lee, J., Zhong, J., and Wright, S. C. (1995) Human CAP18: A novel antimicrobial lipopolysaccharide-binding protein. *Infect. Immun. 63*, 1291–1297.
20. Giacometti, A., Cirioni, O., Ghiselli, R., Mocchegiani, F., Orlando, F., Silvestri, C., Bozzi, A., Di Giulio, A., Luzi, C., Mangoni, M. L.,

Barra, D., Saba, V., Scalise, G., and Rinaldi, A. C. (2006) Interaction of antimicrobial peptide temporin L with lipopolysaccharide in vitro and in experimental rat models of septic shock caused by gram-negative bacteria. *Antimicrob. Agents Chemother. 50*, 2478–2486.

21. Brown, K. L., and Hancock, R. E. (2005) Cationic host defense (antimicrobial) peptides. *Curr. Opin. Immunol. 18*, 24–30.
22. Castano, S., Cornut, I., Buttner, K., Dasseux, J. L., and Dufourcq, J. (1999) The amphipathic helix concept: Length effects on ideally amphipathic LiKj(*i*=2j) peptides to acquire optimal hemolytic activity. *Biochim. Biophys. Acta 1416*, 161–175.
23. Beven, L., Castano, S., Dufourcq, J., Wieslander, A., and Wroblewski, H. (2003) The antibiotic activity of cationic linear amphipathic peptides: Lessons from the action of leucine/lysine copolymers on bacteria of the class Mollicutes. *Eur. J. Biochem. 270*, 2207–2217.
24. Pouny, Y., and Shai, Y. (1992) Interaction of D-amino acid incorporated analogues of pardaxin with membranes. *Biochemistry 31*, 9482–9490.
25. Rapaport, D., and Shai, Y. (1991) Interaction of fluorescently labeled pardaxin and its analogues with lipid bilayers. *J. Biol. Chem. 266*, 23769–23775.
26. de Haas, C. J., van Leeuwen, H. J., Verhoef, J., van Kessel, K. P., and van Strijp, J. A. (2000) Analysis of lipopolysaccharide (LPS)-binding characteristics of serum components using gel filtration of FITC-labeled LPS. *J. Immunol. Methods 242*, 79–89.
27. Oren, Z., and Shai, Y. (2000) Cyclization of a cytolytic amphipathic α-helical peptide and its diastereomer: Effect on structure, interaction with model membranes, and biological function. *Biochemistry 39*, 6103–6114.
28. Tamm, L. K., and Tatulian, S. A. (1997) Infrared spectroscopy of proteins and peptides in lipid bilayers. *Q. Rev. Biophys. 30*, 365–429.
29. Greenfield, N., and Fasman, G. D. (1969) Computed circular dichroism spectra for the evaluation of protein conformation. *Biochemistry 8*, 4108–4116.
30. Wu, C. S., Ikeda, K., and Yang, J. T. (1981) Ordered conformation of polypeptides and proteins in acidic dodecyl sulfate solution. *Biochemistry 20*, 566–670.
31. Meng, F. G., Zeng, X., Hong, Y. K., and Zhou, H. M. (2001) Dissociation and unfolding of GCN4 leucine zipper in the presence of sodium dodecyl sulfate. *Biochimie 83*, 953–956.
32. Opal, S. M., Scannon, P. J., Vincent, J. L., White, M., Carroll, S. F., Palardy, J. E., Parejo, N. A., Pribble, J. P., and Lemke, J. H. (1999) Relationship between plasma levels of lipopolysaccharide (LPS) and LPS-binding protein in patients with severe sepsis and septic shock. *J. Infect. Dis. 180*, 1584–1589.
33. Frey, S., and Tamm, L. K. (1990) Membrane insertion and lateral diffusion of fluorescence-labelled cytochrome c oxidase subunit IV signal peptide in charged and uncharged phospholipid bilayers. *Biochem. J. 272*, 713–719.
34. Gutsmann, T., Fix, M., Larrick, J. W., and Wiese, A. (2000) Mechanisms of action of rabbit CAP18 on monolayers and liposomes made from endotoxins or phospholipids. *J. Membr. Biol. 176*, 223–236.
35. Papo, N., and Shai, Y. (2005) A molecular mechanism for lipopolysaccharide protection of Gram-negative bacteria from antimicrobial peptides. *J. Biol. Chem. 280*, 10378–10387.
36. Avrahami, D., and Shai, Y. (2002) Conjugation of a magainin analogue with lipophilic acids controls hydrophobicity, solution assembly, and cell selectivity. *Biochemistry 41*, 2254–2263.
37. Avrahami, D., and Shai, Y. (2004) A new group of antifungal and antibacterial lipopeptides derived from non-membrane active peptides conjugated to palmitic acid. *J. Biol. Chem. 279*, 12277–12285.
38. Jackson, M., and Mantsch, H. H. (1995) The use and misuse of FTIR spectroscopy in the determination of protein structure. *Crit. Rev. Biochem. Mol. Biol. 30*, 95–120.
39. Frey, S., and Tamm, L. K. (1991) Orientation of melittin in phospholipid bilayers. A polarized attenuated total reflection infrared study. *Biophys. J. 60*, 922–930.
40. Oren, Z., Lerman, J. C., Gudmundsson, G. H., Agerberth, B., and Shai, Y. (1999) Structure and organization of the human antimicrobial peptide LL-37 in phospholipid membranes:Relevance to the molecular basis for its non-cell-selective activity. *Biochem. J. 341*, 501–513.
41. Sharon, M., Oren, Z., Shai, Y., and Anglister, J. (1999) 2D-NMR and ATR-FTIR study of the structure of a cell-selective diastereomer of melittin and its orientation in phospholipids. *Biochemistry 38*, 15305–15316.
42. Papo, N., Oren, Z., Pag, U., Sahl, H. G., and Shai, Y. (2002) The consequence of sequence alteration of an amphipathic α-helical antimicrobial peptide and its diastereomers. *J. Biol. Chem. 277*, 33913–33921.
43. Bowdish, D. M., and Hancock, R. E. (2005) Anti-endotoxin properties of cationic host defence peptides and proteins. *J. Endotoxin Res. 11*, 230–236.
44. Merrifield, R. B., Merrifield, E. L., Juvvadi, P., Andreu, D., and Boman, H. G. (1994) Design and synthesis of antimicrobial peptides. *Ciba Found. Symp. 186*, 5–26.
45. Oren, Z., and Shai, Y. (1998) Mode of action of linear amphipathic α-helical antimicrobial peptides. *Biopolymers 47*, 451–463.
46. Shai, Y. (1999) Mechanism of the binding, insertion and destabilization of phospholipid bilayer membranes by α-helical antimicrobial and cell non-selective membrane-lytic peptides. *Biochim. Biophys. Acta 1462*, 55–70.
47. Falla, T. J., Karunaratne, D. N., and Hancock, R. E. (1996) Mode of action of the antimicrobial peptide indolicidin. *J. Biol. Chem. 271*, 19298–19303.
48. Matsuzaki, K., Harada, M., Funakoshi, S., Fujii, N., and Miyajima, K. (1991) Physicochemical determinants for the interactions of magainins 1 and 2 with acidic lipid bilayers. *Biochim. Biophys. Acta 1063*, 162–170.
49. Chen, X., Howe, J., Andra, J., Rossle, M., Richter, W., da Silva, A. P., Krensky, A. M., Clayberger, C., and Brandenburg, K. (2007) Biophysical analysis of the interaction of granulysin-derived peptides with enterobacterial endotoxins. *Biochim. Biophys. Acta 1768*, 2421–2431.
50. Shnyra, A., Hultenby, K., and Lindberg, A. A. (1993) Role of the physical state of *Salmonella* lipopolysaccharide in expression of biological and endotoxic properties. *Infect. Immun. 61*, 5351–5360.
51. Andra, J., Lamata, M., Martinez de Tejada, G., Bartels, R., Koch, M. H., and Brandenburg, K. (2004) Cyclic antimicrobial peptides based on *Limulus* anti-lipopolysaccharide factor for neutralization of lipopolysaccharide. *Biochem. Pharmacol. 68*, 1297–1307.
52. Howe, J., Andra, J., Conde, R., Iriarte, M., Garidel, P., Koch, M. H., Gutsmann, T., Moriyon, I., and Brandenburg, K. (2007) Thermodynamic analysis of the lipopolysaccharide-dependent resistance of gram-negative bacteria against polymyxin B. *Biophys. J. 92*, 2796–2805.
53. Andra, J., Howe, J., Garidel, P., Rossle, M., Richter, W., Leiva-Leon, J., Moriyon, I., Bartels, R., Gutsmann, T., and Brandenburg, K. (2007) Mechanism of interaction of optimized *Limulus*-derived cyclic peptides with endotoxins: Thermodynamic, biophysical and microbiological analysis. *Biochem. J. 406*, 297–307.

BI800450F